J. Electrochem. Sci. Eng. **15(3)** (2025) 2627; http://dx.doi.org/10.5599/jese.2627

Open Access : : ISSN 1847-9286
www.jESE-online.org

Original scientific paper

Electrochemical modulation of annealed steel *via* cupric sulfate, potassium chloride and trisodium citrate: insights into redox behaviour and corrosion resistance

Francisco Augusto Nuñez Perez✉

Maestría en Ciencias en Ingeniería, Universidad Politécnica de Lázaro Cárdenas, Michoacán C.P. 60998, Mexico

Corresponding author: ✉*augusto@uplc.edu.mx; Tel.: +52-753-136-4242*

Received: January 3, 2025; Accepted: April 4, 2025; Published: April 29, 2025

Abstract

This study probes the electrochemical modulation of annealed steel in 0.01 M copper sulfate ($CuSO_4$) solutions with potassium chloride (KCl) and trisodium citrate additives, using cyclic voltammetry, electrochemical impedance spectroscopy and chronoamperometry. A three-electrode system, annealed steel wire, Ag/AgCl reference and Pt counter electrode, evaluated pure $CuSO_4$, $CuSO_4$ with 0.01 M KCl and $CuSO_4$ with 0.01 M trisodium citrate. KCl amplifies current density by 123 % and reduces charge transfer resistance by 75 % at -0.8 V vs. Ag/AgCl, enhancing copper electrodeposition kinetics. Trisodium citrate, forming Cu^{2+} complexes, curtails redox activity by 51 % and elevates polarization resistance at -0.6 V, fostering passivation. Measurements at -0.6 and -0.8 V highlight kinetic dominance of KCl and stabilizing effect of citrate ions, slashing corrosion rates from 154.87 to 8.05 mm $year^{-1}$. These insights make a framework for corrosion-resistant coatings without reliance on structural imaging, with broad implications for electrochemical applications.

Keywords

Electrolysis; morphology; crystal orientation; scanning electron microscopy, X-ray diffraction

Introduction

Electrochemical systems involving metallic interfaces are fundamental to a wide range of technological applications, spanning energy storage and conversion, corrosion protection, and the development of advanced coatings [1]. Among these, steel and copper-based systems hold particular relevance due to their widespread industrial use and the unique redox characteristics of copper species [2]. Annealed steel was selected as the working electrode to investigate copper electrodeposition as a strategy for enhancing corrosion resistance of ferrous substrates relevant for industrial applications. The dynamics of copper electrodeposition and corrosion on steel surfaces play a pivotal role in controlled electrodeposition, electrocatalysis, and the design of anticorrosive coatings [3].

However, the precise control of these processes requires a detailed understanding of how electrolytic conditions and chemical additives influence redox dynamics and interfacial properties [4].

Copper sulfate ($CuSO_4$) is widely used as a precursor in electrodeposition systems due to its high solubility and well-characterized redox properties [5]. However, the intrinsic limitations of pure $CuSO_4$ solutions, such as diffusional restrictions and relatively high charge transfer resistance, necessitate the use of additives to optimize their performance [6]. Among the most studied additives are potassium chloride (KCl) and trisodium citrate dihydrate ($Na_3C_6H_5O_7{\cdot}2H_2O$), due to their contrasting effects on the electrochemical behaviour of cupric species [7]. KCl enhances electrochemical conductivity and facilitates charge transfer by providing chloride ions (Cl^-), which stabilize transient copper complexes of Cu^+ and Cu^{2+} ions. The coordination between Cl^- and copper ions allows the formation of Cu-Cl species in the electrochemical environment, which decouples redox reactions into two stages: Cu^{2+}/Cu^+ and Cu^+/Cu^0. This stabilization not only reduces the electrode negative potential but also improves redox kinetics, increasing charge transfer efficiency and system conductivity [8]. Meanwhile, citrate acts as a chelating agent, stabilizing cupric ions and modulating their reactivity [9]. However, a systematic and comparative analysis of their influence on copper deposition and corrosion behaviour, particularly on annealed steel electrodes, remains an underexplored area.

Furthermore, the electrochemical behaviour of copper electrodeposition systems in copper sulfate solutions in the presence of additives such as KCl and trisodium citrate, is strongly determined by the applied potential. Several studies have reported that, within certain potential ranges, metal deposition is influenced by a balance between kinetic and diffusional control, which is critical for the quality of the resulting coating [10]. Specifically, the potential range between -0.6 and -0.8 V *vs*. Ag/AgCl is of particular interest, as it encompasses regions where the deposition rate is limited by the diffusive transport of metal ions to the cathode, as well as regions where nucleation and growth kinetics govern the electrochemical process [11]. Despite its potential applicability in optimizing industrial coatings, the underlying mechanisms and the formation of intermediate species, such as Cu(I) [12], have yet to be fully characterized within this potential range.

This lack of understanding prevents the precise optimization of key parameters, such as current density, solution pH, and the type of additives, which are critical for controlling the functional properties of deposited coatings. Further investigation in this area presents a significant research opportunity to develop more efficient and robust electrochemical strategies, particularly for applications where corrosion resistance and coating quality are essential requirements [13].

The electrochemical behaviour of an annealed steel wire electrode was investigated in $CuSO_4$ solutions under three distinct conditions: (i) $CuSO_4$ alone, (ii) $CuSO_4$ with KCl and (iii) $CuSO_4$ with trisodium citrate. Using techniques such as cyclic voltammetry, electrochemical impedance spectroscopy, and chronoamperometry, the impact of these additives on charge transfer kinetics, corrosion resistance, and copper deposition was systematically evaluated. The results revealed the synergistic effects of KCl in enhancing deposition efficiency and the stabilizing role of citrate in controlling redox dynamics, providing a comprehensive framework for tailoring steel-copper systems to specific applications [14]. This work not only offers fundamental insights into the electrochemical interactions between additives and copper species but also lays the groundwork for designing advanced materials and optimized processes for electrodeposition, corrosion protection, and catalytic applications.

Experimental

An electrochemical cell configured with three electrodes was employed in this study. The working electrode, an annealed steel wire, was mechanically polished with 600-grit sandpaper, cleaned in

0.1 M HCl for 30 s to remove oxides, then rinsed with deionized water and air-dried, yielding a geometrically verified active area of 0.0201 cm^2. A platinum electrode was used as the counter electrode due to its excellent conductivity and chemical stability in aggressive media [15,16], while the reference electrode was an Ag/AgCl (Metrohm, 6.0733.100) filled with 3 mol L^{-1} KCl solution, widely recognized for its reliability and stability in electrochemical measurements. All solutions were prepared with deionized water and analytical-grade reagents.

Experimental conditions

Pure copper sulfate ($CuSO_4$, 0.01 M): this solution was employed as a reference system to characterize Cu^{2+} electrodeposition and corrosion of the ferrous substrate without additive interference. The electrolyte was prepared using anhydrous $CuSO_4$ (Sigma-Aldrich, ≥99.99 % trace metals basis purity), dissolved in deionized water to 0.01 M, resulting in an initial conductivity of 965 µS cm^{-1} (25 ± 1 °C, measured with a Mettler Toledo SevenExcellence conductometer). This concentration was selected to ensure a controlled diffusion regime, avoiding pH effects associated with acidic H_2SO_4 commonly used in similar systems.

Copper sulfate with KCl (0.01 M $CuSO_4$ + 0.01 M KCl): potassium chloride (KCl, Sigma-Aldrich, Primary Standard grade) was incorporated at 0.01 M to investigate the role of Cl^- ions in charge transfer and copper nucleation. The initial conductivity reached 2153 µS cm^{-1}, reflecting an increased density of ionic charge carriers (K^+ and Cl^-), a well-documented effect that reduces ohmic resistance and enhances interfacial kinetics.

Copper sulfate with trisodium citrate (0.01 M $CuSO_4$ + 0.01 M $Na_3C_6H_5O_7 \times 2H_2O$): trisodium citrate dihydrate (99.0-101.0% (by non aqueous titration), granular, BAKER ANALYZED® ACS, J.T.Baker® - https://www.avantorsciences.com/in/en/product/17899497/tri-sodium-citrate-dihydrate-99-0-101-0-by-non-aqueous-titration-granular-baker-analyzed-acs-j-t-baker) was added at 0.01 M as a chelating agent to stabilize Cu^{2+} and modulate redox dynamics. The initial conductivity recorded 2534 µS cm^{-1}, a consequence of $Na_3C_6H_5O_7$ dissociation into three Na^+ ions and the citrate anion, enhancing ionic mobility and altering the electrical double-layer structure at the electrode-electrolyte interface.

Additive concentrations were fixed at 0.01 M to maintain stoichiometric consistency with $CuSO_4$, facilitating the deconvolution of their electrochemical contributions. Initial conductivities, reported in Table 1, were measured in triplicate (standard deviation <2 %) and reflect the intrinsic properties of each electrolyte prior to electrochemical testing. These values constitute a critical parameter for interpreting charge transfer and diffusion kinetics, as elaborated in the Results and Discussion section.

Electrochemical techniques

All electrochemical experiments were conducted at 25 ± 1 °C using solutions prepared as described above. Before electrochemical measurements, the electrode was stabilized under open-circuit potential (OCP) for 60 seconds. This step does not prevent the spontaneous displacement reaction ($Fe^0 + Cu^{2+} \rightarrow Fe^{2+} + Cu^0$), which is thermodynamically inevitable. Instead, it allows the system to reach a pseudo-steady state prior to applying a controlled potential. This approach ensures that the subsequent electrochemical responses arise from the applied polarization rather than from uncontrolled displacement.

Cyclic voltammetry (CV) was performed using a potentiostat/galvanostat (Metrohm Autolab model) under a potential range of -1.2 to 0.4 V *vs*. Ag/AgCl, with a scan rate of 0.01 V s^{-1}. The obtained

voltammograms allowed analysis of the redox processes and copper deposition under different experimental conditions.

Electrochemical impedance spectroscopy (EIS) experiments were conducted at fixed potentials of -0.6 and -0.8 V *vs.* Ag/AgCl, covering a frequency range of 100 kHz to 0.1 Hz with a perturbation amplitude of 10 mV. The data were represented in Nyquist and Bode plots, and modeled using equivalent circuits to evaluate charge transfer resistance (R_{ct}) and diffusion limitations.

Chronoamperometry (CA) was applied at constant potentials of -0.6 and -0.8 V *vs*. Ag/AgCl to evaluate the nucleation and growth kinetics of the copper deposit. The data provided transient and stable current responses under each condition.

Copper coatings were electrodeposited onto annealed steel electrodes (0.0201 cm² active area) at constant potentials of -0.6 and -0.8 V *vs*. Ag/AgCl. The deposition time was 120 seconds for all samples, as established by chronoamperometry.

Tafel curves were derived from the obtained voltammograms and used to calculate parameters such as corrosion current density (j_{corr}), corrosion potential (E_{corr}) and polarization resistance (R_p) [17].

To experimentally verify the theoretical coating thickness calculated using Faraday's law, gravimetric measurements were performed following chronoamperometric copper deposition. The coated electrodes were gently rinsed with deionized water, dried at room temperature, and weighed using an OHAUS Explorer® EX125 analytical microbalance with a readability of ±0.01 mg. The mass difference before and after deposition, normalized to the electrode area (0.0201 cm²), was used to calculate the coating thickness based on the known density of copper (8.96 g cm^{-3}). All gravimetric measurements were performed in triplicate under identical deposition parameters (potential, time, and active area) to ensure consistency with the corresponding electrochemical tests.

Results and discussion

Prior to initiating controlled electrochemical measurements, the annealed steel electrode was stabilized in each 0.01 M solution ($CuSO_4$, $CuSO_4$ + KCl, $CuSO_4$ + $Na_3C_6H_5O_7\times2H_2O$) under OCP for a maximum of 60 seconds to account for the spontaneous displacement reaction, Equation (1):

$$Fe^0 + Cu^{2+} \rightarrow Fe^{2+} + Cu^0 \quad (1)$$

with standard reduction potentials ($E°$) of corresponding electrode reactions: $E°(Cu^{2+}/Cu^0)$ ≈ ≈ 0.137 V *vs.* Ag/AgCl (saturated KCl), and $E°(Fe^{2+}/Fe^0)$ ≈ -0.637 V *vs.* Ag/AgCl (saturated KCl)

This thermodynamically favored process reflects the baseline electrochemical interaction at the steel surface under stationary conditions, where iron dissolution (anodic: $Fe^0 \rightarrow Fe^{2+} + 2e^-$) drives copper deposition (cathodic: $Cu^{2+} + 2e^- \rightarrow Cu^0$). These reactions establish the initial state of the system, which is subsequently modulated under polarization, as explored in the following analyses. The OCP stabilization isolates controlled electrodeposition and corrosion kinetics from spontaneous interfacial processes, underpinning the quantitative characterization summarized in Table 1.

Table 1. Electrochemical properties of 0.01 M solutions before and after chronoamperometry

Solution	Potential, V	OCP, V	Conductivity, μS cm^{-1}		
			Initial	After chronoamperometry	Change
Only copper sulfate	-0.8	-0.3030	965	936	29
	-0.6	-0.3000	965	941	24
Copper sulfate with KCl	-0.8	-0.5713	2153	2143	10
	-0.6	-0.5720	2153	2140	13
Copper sulfate with trisodium citrate	-0.8	-0.6190	2534	2524	10
	-0.6	-0.6090	2534	2618	-84

The open-circuit potentials recorded prior to polarization revealed a progressive cathodic shift in the presence of KCl and citrate, consistent with Cu^{2+} complexation by Cl^- and citrate ligands. These species are known to form transient $CuCl^+$ and stable $[Cu(C_6H_5O_7)]^-$ complexes, which modify interfacial redox behaviour and promote Fe dissolution. Similarly, the increase in initial conductivity upon additive incorporation reflects enhanced ionic mobility, a key factor influencing charge transfer kinetics. These preliminary measurements, summarized in Table 1 and validated through triplicate experiments, establish the electrochemical baseline for subsequent chronoamperometric and EIS analyses.

Cyclic voltammetry plots

Cyclic voltammograms obtained at a scan rate of 0.01 V s^{-1} using an annealed steel electrode in $CuSO_4$ solution with and without additives (KCl and trisodium citrate dihydrate) are presented in Figure 1. Under polarization (potential range from -1.2 to 0.4 V *vs.* Ag/AgCl), the system exhibits two primary electrode processes: the cathodic reduction of Cu^{2+} to Cu^0 ($Cu^{2+} + 2e^- \rightarrow Cu^0$) and the anodic oxidation of Fe^0 to Fe^{2+} ($Fe^0 \rightarrow Fe^{2+} + 2e^-$). The polarization dependencies reflect the combined kinetics of these reactions, modulated by the presence of additives, as detailed below.

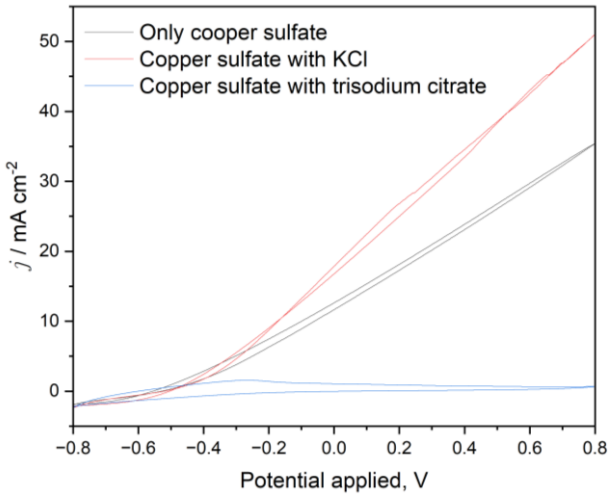

Figure 1. *Cyclic voltammetry of annealed steel electrode in copper sulfate solution without and with KCl and trisodium citrate additives at a scan rate of 0.01 V s^{-1}*

As shown by the black curve in Figure 1, the electrochemical response represents the baseline behaviour, where Cu^{2+} reduction and Fe dissolution occur without interference. The moderate current density indicates diffusional and kinetic limitations inherent to the pure $CuSO_4$ system, where electron transfer and Cu^{2+} reduction kinetics are limited by the intrinsic properties of the electrolyte and the electrode-electrolyte interface.

The red curve in Figure 1 indicates that the addition of potassium chloride (KCl significantly increases cathodic current density. This enhancement results from two main effects: (i) increased ionic conductivity due to the presence of K^+ and Cl^- ions, which lowers solution resistance; and (ii) specific adsorption of Cl^- on the electrode surface, which stabilizes transient $CuCl^+$ species and reduces the overpotential for Cu^{2+} reduction ($Cu^{2+} + 2e^- \rightarrow Cu^0$). Under these conditions, Fe oxidation plays a secondary role compared to the dominant copper deposition pathway. The 123 % increase in conductivity (from 965 to 2153 µS cm^{-1}, Table 1) facilitates charge transport and enhances the kinetics of Cu^{2+} reduction. No significant evidence of Fe dissolution was observed at -0.6 or -0.8 V. The reduced charge transfer resistance, together with the higher current density,

confirms the promoting effect of Cl^- on interfacial electron transfer, as reflected in the voltammetric profile (Figure 1) and previously reported findings [18].

As shown by the curve in Figure 2, the addition of trisodium citrate to the copper sulfate solution marked a decrease in current density, reflecting inhibition of both cathodic and anodic processes, with a stronger effect on Cu^{2+} reduction. Trisodium citrate complexes of Cu^{2+}, such as $[Cu(C_6H_5O_7)]^-$, reducing the availability of free Cu^{2+} for the cathodic reaction ($Cu^{2+} + 2e^- \rightarrow Cu^0$), while surface passivation *via* citrate adsorption limits Fe dissolution ($Fe \rightarrow Fe^{2+} + 2e^-$). This dual suppression leads to attenuated redox peaks.

Citrate acts as a multidentate ligand, coordinating with Cu^{2+} through its carboxylate groups to form stable complexes in solution. This complexation significantly reduces the concentration of redox-active species at the electrode-electrolyte interface and limits charge transfer. Such behavior is consistent with earlier studies on metal-ligand coordination systems and the electrochemical stabilization provided by chelating agents [19].

Additionally, Cu-citrate complexes exhibit reduced electrochemical reactivity compared to free Cu^{2+} ions due to the high activation energy required for complex dissociation prior to electron transfer. This results in a notable decrease in redox peak intensity (Figure 2).

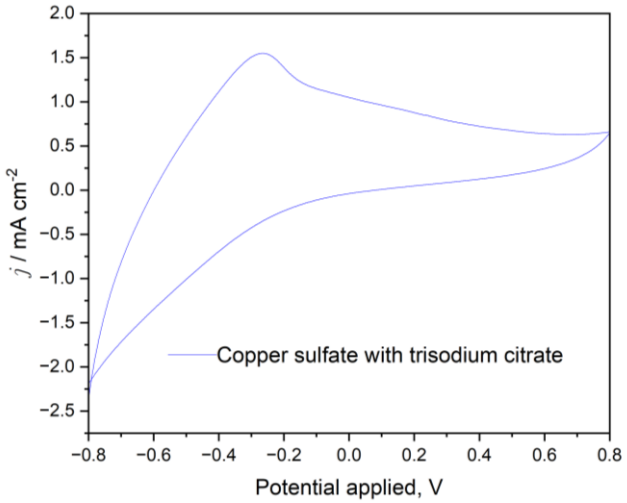

Figure 2. *Cyclic voltammogram of an annealed steel electrode in a copper sulfate solution with trisodium citrate addition at a scan rate of 0.01 V s^{-1}*

Adsorption and surface passivation effects: The presence of citrate in the solution leads to significant adsorption on the annealed steel electrode surface, promoting the formation of a stable passivating layer. This phenomenon is attributed to the high affinity of citrate ions for coordinating with surface atoms through their carboxylate groups, creating a physical barrier that partially blocks active sites. Consequently, direct Cu^{2+} access to the electrode surface is inhibited, limiting mass transfer and reducing the reduction process efficiency. The presence of this passivating layer is consistent with the gradual decrease in current density observed in the voltammograms and has been previously documented in systems where coordinating ligands such as citrate or analogous species modify metal surface reactivity. Peng *et al.* [20] demonstrated that surface coordination layers could act as protective barriers, significantly reducing substrate interaction with the reactive environment. Meanwhile, studies by Nikkhou *et al*. [21] showed that citrate could induce surface passivation in leaching media, altering electrochemical reaction kinetics.

Figures 1 and 2 complementarily illustrate how KCl and trisodium citrate additives modulate the electrochemical activity of the $CuSO_4$ - steel system. KCl enhances electron transfer kinetics and

boosts current through adsorption and transient complexation mechanisms. Conversely, trisodium citrate inhibits electrochemical response through strong Cu^{2+} complexation, slowed kinetics, and surface passivation. These findings underscore the importance of additives in modulating redox processes and provide a fundamental basis for optimizing electrochemical systems in practical applications. The comparison between both figures not only identifies the qualitative effects of the additives but also delves deeper into the underlying mechanisms controlling charge transfer and the availability of redox species.

Charge transfer behaviour and electrodeposition kinetics of copper on annealed steel at -0.8 V, influence of KCl and citrate additives

Figure 3 presents the Nyquist plots obtained for the three solutions evaluated. The experiments were conducted at a constant potential of -0.8 V using a three-electrode system comprising a platinum counter electrode, a silver/silver chloride reference electrode, and an annealed steel wire working electrode. This configuration allows for precise evaluation of the electrochemical properties of each system under controlled conditions.

In the case of the pure copper sulfate solution, the prominent semicircle in the high-frequency region indicates high charge transfer resistance for Cu^{2+} reduction, with diffusion limitations for Cu^{2+} transport evident at low frequencies. The anodic process contributes minimally at this potential due to the strong cathodic overpotential.

Upon addition of potassium chloride to the copper sulfate solution, a significant reduction in the semicircle diameter is observed, indicating lower charge transfer resistance, primarily attributed to the cathodic reaction ($Cu^{2+} + 2e^- \rightarrow Cu^0$). The presence of Cl^- ions enhances the reduction kinetics of Cu^{2+} by forming transient $CuCl^+$ species and adsorbing onto the electrode surface. This not only facilitates electron transfer but also mitigates diffusion limitations through improved ionic transport. Overall, this effect corresponds to a 75 % decrease in charge transfer resistance at -0.8 V *vs.* Ag/AgCl, driven by Cl^- adsorption and enhanced interfacial dynamics.

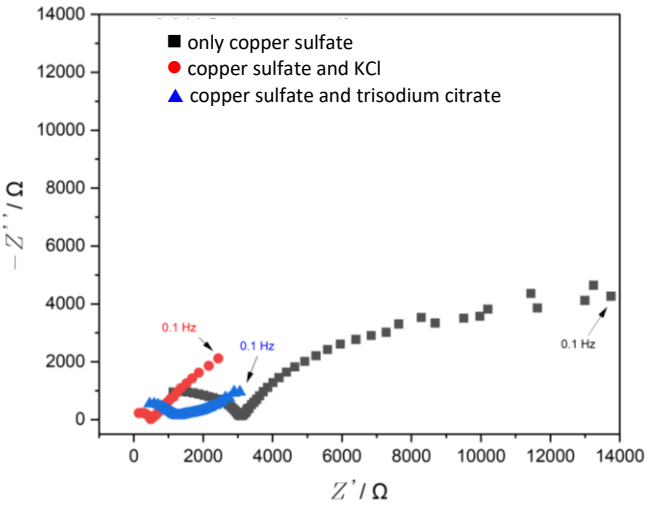

Figure 3. *Nyquist plots evaluating charge transfer resistance at annealed steel in copper sulfate solutions without and with additives (KCl and trisodium citrate) at -0.8 V*

At low frequencies, the slope is less pronounced compared to the pure system, reflecting improved ionic transport due to the increased mobility of species provided by KCl. Additionally, Cl^- ions may adsorb onto the electrode surface, favorably altering the electrical double-layer structure, consistent with previous studies reporting the synergistic effect of Cl^- and other ionic species in reducing charge transfer resistance and modifying the electrode-electrolyte interface [22].

An intermediate-sized semicircle suggests moderate charge transfer resistance, primarily due to suppressed Cu^{2+} reduction ($Cu^{2+} + 2e^- \rightarrow Cu^0$) from citrate complexation ($[Cu(C_6H_5O_7)]^-$). The anodic reaction ($Fe^0 \rightarrow Fe^{2+} + 2e^-$) is also inhibited by surface passivation, contributing to the overall modulated electrochemical response. This modulation curtails redox activity by 51 %, as citrate complexes reduce free Cu^{2+} availability, indicating moderate charge transfer resistance. The formation of stable citrate-copper complexes decreases the concentration of free Cu^{2+} ions available for redox processes, thus modulating electrochemical kinetics. At low frequencies, the inclined slope reflects modulated diffusion limitations due to citrate complexation with Cu^{2+} as $[Cu(C_6H_5O_7)]^-$, reducing free Cu^{2+} availability and altering charge transfer dynamics, as evidenced by the intermediate semicircle in Figure 3 (-0.8 V), affecting both Cu^{2+} availability and the double-layer structure [23].

Figure 4 displays the impedance magnitude and phase angle as functions of frequency. This representation provides detailed information about the dominant mechanisms across different frequency scales under identical conditions at -0.8 V.

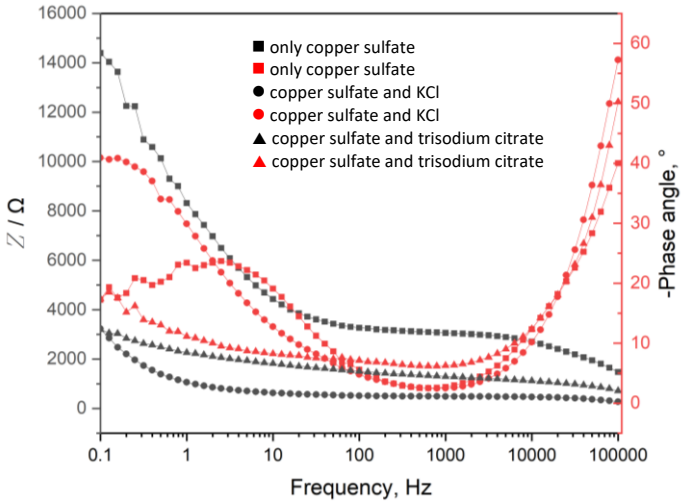

***Figure 4**. Bode plots: Impedance magnitude (black curves) and phase angle (red curves) as a function of frequency at -0.8 V for annealed steel in different copper sulfate systems without and with additives (KCl and trisodium citrate)*

At high frequencies, all systems converge to similar impedance values, primarily reflecting the ohmic resistance of the electrolyte. This confirms that processes associated with charge transfer and diffusion have minimal influence in this range [24]. At medium frequencies, the phase angle peak is most pronounced in the pure copper sulfate system, indicating that charge transfer processes dominate and are decoupled from diffusion processes. Conversely, the KCl system exhibits a lower peak, reflecting a significant improvement in charge transfer efficiency. For the trisodium citrate system, the phase peak is moderate, suggesting that the system operates under a balance between charge transfer and mass transport [25]. At low frequencies, the KCl system exhibits the lowest impedance, confirming a substantial enhancement in ionic transport and reduction kinetics, attributed to the improved mobility of ionic species in the presence of Cl^- [26]. The pure copper sulfate system maintains high impedance, emphasizing its diffusive limitations due to the absence of additives facilitating ionic mobility. For the trisodium citrate system, an intermediate resistance is observed, associated with citrate adsorption on the electrode surface. This adsorption affects the structure of the electrical double layer, introducing a barrier that modulates both the availability of Cu^{2+} ions and the kinetics of redox processes [28].

Figure 5 presents chronoamperometric curves obtained under identical conditions at -0.8 V, allowing evaluation of the nucleation and growth kinetics of the copper deposit.

Pure copper sulfate: The initial current is low and rapidly decreases to stable values, which are also low. This reflects the high charge transfer resistance and inherent diffusive limitations of the system. This behaviour is driven by high charge transfer resistance and diffusion limitations in pure $CuSO_4$, as indicated by the low initial current and rapid stabilization at reduced values (Figure 5), consistent with the large semicircle in Figure 3.

Copper sulfate with KCl: This system shows the highest and most stable currents throughout the experiment, indicating rapid and efficient electrodeposition kinetics. The presence of KCl not only improves charge transfer but also minimizes diffusive limitations by increasing the mobility of ionic species. This enables uniform and accelerated deposit growth.

Copper sulfate with trisodium citrate: The initial current is lower than that of the KCl system but higher than that of the pure sulfate. The gradual decrease in current suggests more controlled electrodeposition, attributable to complex formation between citrate and copper species. This system is ideal for applications requiring uniform deposits, albeit with slower growth rates.

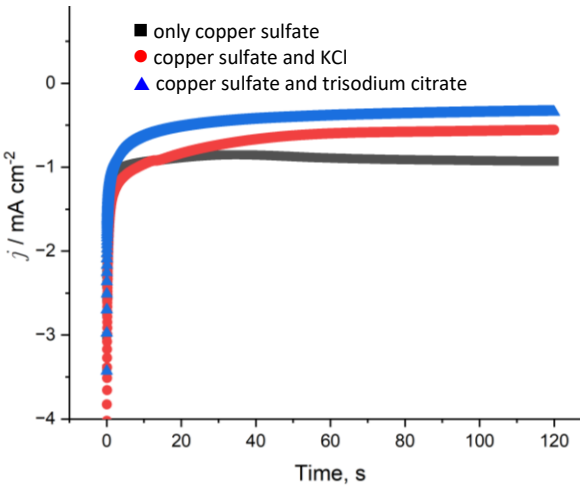

Figure 5. *Chronoamperometric curves for copper electrodeposition at -0.8 V in pure copper sulfate, KCl-added, and trisodium citrate-added solutions*

The identification of the limiting processes in Table 2 was not based on equivalent circuit modeling, but rather on comparative analysis of experimental data obtained from electrochemical impedance spectroscopy (EIS) and chronoamperometry. For instance, in the Nyquist plots, the diameter of the semicircle is indicative of charge transfer resistance: a larger semicircle (*e.g.* pure $CuSO_4$) suggests kinetic control, whereas a smaller semicircle (*e.g.* $CuSO_4$ + KCl) indicates enhanced kinetics and reduced resistance. Similarly, chronoamperometric curves that quickly stabilize suggest kinetically controlled processes, while steep decays are characteristic of diffusion limitation. These combined experimental indicators were considered sufficient to identify the dominant limitation without requiring numerical simulation or circuit fitting.

The chronoamperometric and electrochemical impedance spectroscopy (EIS) data exhibit strong concordance, jointly elucidating the electrochemical processes occurring in each system at -0.8 V. In the presence of KCl, the lowest charge transfer resistance is observed, reflecting a significant improvement in electrodeposition kinetics and ionic species mobility [27]. On the other hand, trisodium citrate reduces the availability of Cu^{2+} ions through complexation and generates surface adsorption, resulting in intermediate resistance and a more controlled process. The pure copper sulfate system exhibits the highest resistance, highlighting the intrinsic limitations of the redox

process in the absence of additives. These results, obtained at a constant potential of -0.8 V, underline the impact of additives in optimizing charge transfer and modulating the electrochemical activity of the $CuSO_4$ system.

Table 2. *Quantitative summary of charge transfer resistance and the limiting processes observed for each system evaluated at a constant potential of -0.8 V*

Solution	Charge transfer resistance	Limiting processes
Only copper sulfate	Highest	Charge transfer resistance dominates.
Copper sulfate with KCl	Lowest	Moderate ohmic resistance and enhanced ion mobility.
Copper sulfate with trisodium citrate	Intermediate	Complexation of Cu^{2+} and slower diffusion kinetics.

Charge transfer behavior and electrodeposition kinetics of copper on annealed steel at -0.6 V influence of KCl and citrate additives

Figure 6 presents the Nyquist plots obtained at a constant potential of -0.6 V. This potential, more positive than -0.8 V, significantly modifies the electrochemical processes, particularly the charge transfer resistance and diffusional limitations.

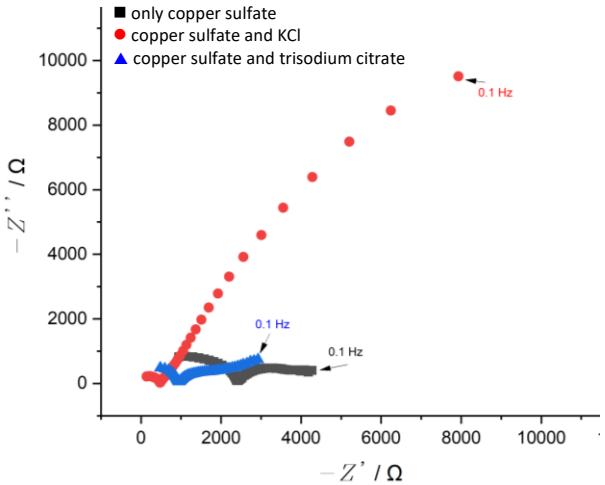

Figure 6. *Nyquist plots evaluating charge transfer resistance at annealed steel in copper sulfate solutions with and without additives (KCl and trisodium citrate) at -0.6 V*

Pure copper sulfate: The semicircle in the high-frequency region is less pronounced compared to measurements at -0.8 V, suggesting a slight decrease in charge transfer resistance. However, diffusional limitations remain dominant, as indicated by the inclined curve at low frequencies. This behaviour reflects that at -0.6 V, the Cu^{2+} reduction kinetics are still limited, albeit less severe than at more negative potentials, due to a lower overpotential.

Copper sulfate with KCl: The reduction in the semicircle diameter is even more notable compared to the pure system. This confirms that Cl^- ions significantly enhance charge transfer by lowering the energy barrier for Cu^{2+} reduction. At low frequencies, the less pronounced slope indicates an effective reduction in diffusional limitations, a result of KCl ability to increase the ionic strength of the solution and facilitate species transport.

Copper sulfate with trisodium citrate: The system with citrate exhibits a semicircle intermediate between the pure sulfate and the KCl system, indicating moderate charge transfer resistance. At low frequencies, the curve reveals modulated diffusional limitations due to the formation of complexes

between citrate and Cu^{2+}. These complexes reduce the availability of free ions for redox processes, slowing reduction kinetics but allowing more uniform control of transport processes.

Figure 7 presents Bode plots, which show impedance magnitude (*Z*) and phase angle as a function of frequency for the annealed steel in three evaluated solutions at a constant potential of -0.6 V. This analysis identifies the predominant mechanisms in different frequency ranges and how they are influenced by additives like KCl and trisodium citrate.

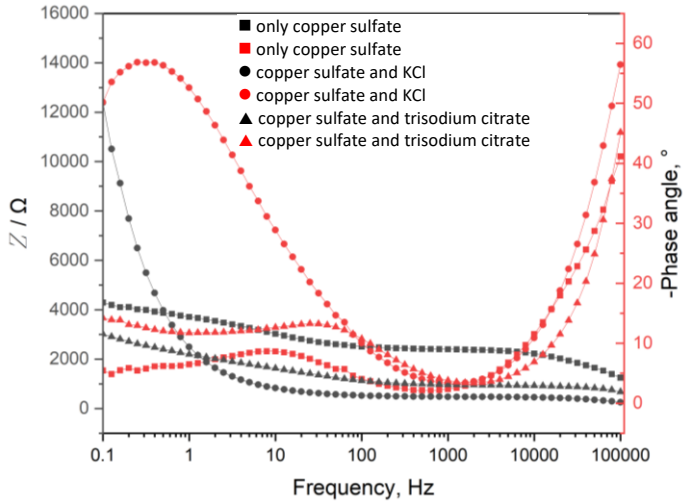

Figure 7. *Bode plots: impedance magnitude (black curves) and phase angle (red curves) as a function of frequency at -0.6 V for annealed steel in different copper sulfate systems with and without additives (KCl and trisodium citrate)*

High frequencies (100,000 to 10,000 Hz): All systems converge to similar impedance values, reflecting the ohmic resistance of the electrolyte. This indicates that charge transfer and diffusion processes have minimal influence in this range.

Medium frequencies (10,000 to 10 Hz): The phase angle peak is lower than at -0.8 V, particularly in the KCl system. This indicates that charge transfer is more efficient at -0.6 V, as the reduced overpotential favors faster redox kinetics. For the citrate system, the phase peak is moderate, showing a balance between charge transfer and diffusional limitations.

Low frequencies (10 to 0.1 Hz): The KCl system stands out with the lowest impedance, reflecting high efficiency in charge transfer and optimized ionic transport. In contrast, the citrate system exhibits intermediate behaviour, while the pure sulfate system maintains high impedance, confirming its inherent limitations.

The chronoamperometric curves in Figure 8 were obtained at -0.6 V. Pure copper sulfate: The initial current is higher than at -0.8 V, indicating improved electrodeposition kinetics due to the lower overpotential. However, the current decays rapidly and stabilizes at a low value, reflecting that diffusion limitations and charge transfer resistance remain dominant factors.

Copper sulfate with KCl: The initial current is significantly higher and remains stable throughout the experiment. This confirms that KCl enhances both charge transfer and ionic transport, enabling efficient Cu^{2+} electrodeposition even at a less negative potential.

Copper sulfate with trisodium citrate: The initial current lies between the pure system and the one with KCl. The gradual current decrease reflects the influence of stable complex formation between citrate and Cu^{2+}, which slows the electrodeposition kinetics but facilitates a more uniform deposit growth.

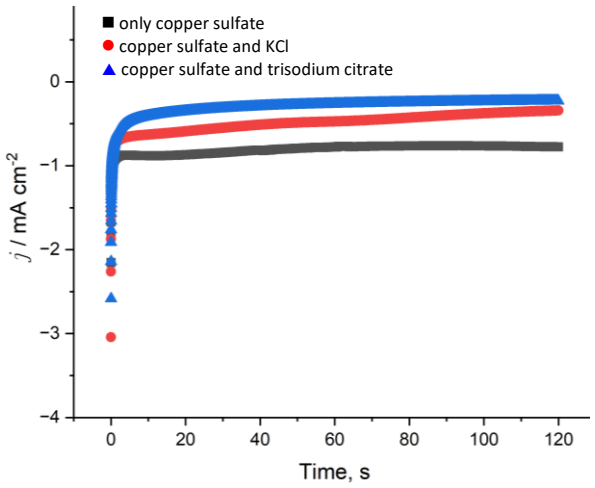

Figure 8. *Chronoamperometric curves for copper electrodeposition at -0.6 V in pure copper sulfate solutions, with KCl, and with trisodium citrate*

Comparative analysis of charge transfer and deposition behaviour at -0.6 V and -0.8 V

At both potentials (-0.6 and -0.8 V), KCl proves to be the most effective additive for enhancing the electrochemical properties of the system. KCl significantly reduces charge transfer resistance, as evidenced by the smaller semicircles in Nyquist plots. Additionally, it improves ionic transport and facilitates efficient electrodeposition of Cu^{2+}. In the chronoamperometric curves, its effect is evident in the higher and more stable initial currents compared to the other systems. At -0.8 V, the higher overpotential amplifies the charge transfer efficiency, while at -0.6 V, the effect remains notable but is moderated by the lower overpotential.

Trisodium citrate modulates charge transfer and diffusion processes through the formation of stable complexes. This behaviour is particularly evident in the slope of the Nyquist plots and the gradual transition in the chronoamperometric curves. At -0.8 V, the formation of complexes reduces the concentration of free ions available for reduction, resulting in lower currents and more controlled deposit growth. At -0.6 V, this effect persists but is slightly diminished due to the system's lower energy demands. In both cases, citrate is ideal for applications requiring uniform and well-controlled deposits.

Pure copper sulfate serves as a reference system, highlighting intrinsic limitations at both potentials. At -0.8 V, it exhibits high charge transfer resistance and severe diffusion limitations, leading to low initial currents and inefficient electrodeposition. These limitations are reflected in the large semicircles in Nyquist plots and high impedance observed in low-frequency Bode diagrams. At -0.6 V, while the limitations are slightly reduced due to the lower overpotential, the system's performance remains inferior compared to systems with additives.

Corrosion protection of annealed steel by copper coatings

The following section assesses the corrosion resistance of electrodeposited copper coatings on annealed steel electrodes, evaluating their effectiveness as a protective barrier against anodic dissolution of the ferrous substrate ($Fe^0 \rightarrow Fe^{2+} + 2e^-$) in 0.01 M $CuSO_4$-based electrolytes, with and without additives (KCl, trisodium citrate). Samples were prepared *via* chronoamperometric deposition at -0.6 and -0.8 V for 120 seconds each, as shown in Figures 5 and 8, yielding coatings of 1.31 to 4 µm based on Faraday's law calculations (see Table 3). Otherwise, Table 3 presents chronoamperometric parameters of copper electrodeposition, including thicknesses of copper coatings.

To validate the theoretical thickness estimates of copper coatings calculated using Faraday's law, a direct gravimetric analysis of the deposited copper layers was performed under identical

experimental conditions (potential, time and active area). The results are shown in the "Thickness gravimetry" column of Table 3. The values of j_{prom} *and* Q values in Table 3 are the average current density over 120 s, and total charge transferred during electrodeposition, defined by Equations (2) and (3), respectively:

$$j_{prom} = \frac{1}{n}\sum_{i=1}^{n} j_i \quad (2)$$

$$Q = \int_0^t j(t)\,dt \quad (3)$$

The thickness (d) was calculated using Equation (4):

$$d = \frac{|Q|M}{nF\rho}10{,}000 \quad (4)$$

where M = 63.546 g mol^{-1} (molar mass of copper), n = 2 (electrons transferred per Cu^{2+} ion), F = 96,485 C mol^{-1} (Faraday constant), and ρ = 8.96 g cm^{-3} (density of copper).

In all cases, the gravimetrically measured thicknesses were significantly lower than the calculated values, confirming current efficiency was below 100 %.

***Table 3**. Chronoamperometric parameters for copper electrodeposition on annealed steel*

Solution	Potential, V	j_{prom} / mA cm^{-2}	Q / mC cm^{-2})	Thickness, µm	Thickness gravimetry, µm
Only copper sulfate	-0.8	-0.910	-109.2	4.013	1.168
Only copper sulfate	-0.6	-0.803	-96.4	3.544	1.073
Copper sulfate with KCl	-0.8	-0.693	-83.1	3.055	0.683
Copper sulfate with KCl	-0.6	-0.483	-57.9	2.130	0.245
Copper sulfate with trisodium citrate	-0.8	-0.448	-53.8	1.978	0.231
Copper sulfate with trisodium citrate	-0.6	-0.297	-35.6	1.311	0.214

The chronoamperometric parameters in Table 3 quantify the copper electrodeposition kinetics on annealed steel under the evaluated conditions. For pure $CuSO_4$ at -0.8 V, the highest average current density (j_{prom} = -0.910 mA cm^{-2}) and charge transferred (Q = -109.2 mC cm^{-2}) result in a deposit thickness of 4.01 µm, reflecting a diffusion-limited process consistent with the rapid current decay observed in Figure 5. At -0.6 V, these values decrease (j_{prom} = -0.804 mA cm^{-2}, Q = -96.4 mC cm^{-2}, thickness = 3.54 µm), indicating reduced overpotential and slower kinetics. The addition of KCl enhances electrodeposition efficiency, reducing Q to -83.1 mC cm^{-2} at -0.8 V (thickness = 3.06 µm) and -58.0 mC cm^{-2} at -0.6 V (thickness = 2.13 µm), despite lower j_{prom} values (-0.693 and -0.483 mA cm^{-2}, respectively). This suggests improved nucleation and growth dynamics due to Cl^- induced over-potential reduction, as evidenced by the stable currents in Figure 5. Conversely, trisodium citrate sup-presses deposition, with Q values of -53.8 mC cm^{-2} at -0.8 V (thickness = 1.98 µm) and -35.7 mC/cm^2 at -0.6 V (thickness = 1.31 µm), reflecting complexation of Cu^{2+} ions that limits free redox species availability, aligning with the gradual current decline in Figure 5. These quantitative differences underscore a role of KCl in accelerating deposition kinetics and the capacity of citrate ions for controlled, uniform coating formation, critical for optimizing corrosion-resistant layers.

Linear sweep voltammograms and Tafel curves presented in Figures 9 to 12 detail the redox dynamics and corrosion behaviour of copper-coated annealed steel systems (Fe-Cu systems), highlighting the protective role of copper layers compared to bare steel (E_{corr} = -0.874 V, corrosion rate = 154.87 mm year^{-1}, Table 4).

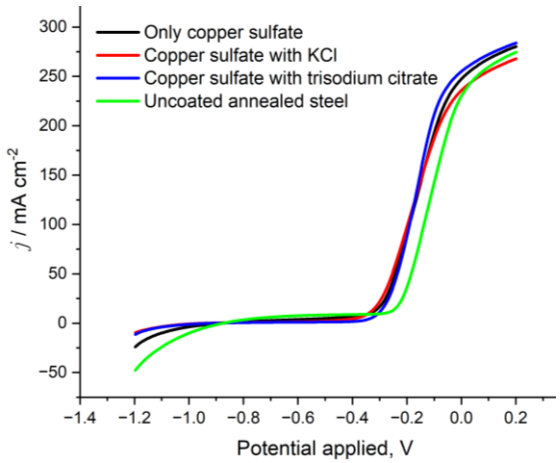

Figure 9. *Linear sweep voltammograms of Fe-Cu system in copper sulfate solutions with and without additives. The electrodes were previously electrodeposited at -0.8 V for 120 s*

The black line in Figure 9 represents the system with pure copper sulfate solution, establishing the electrochemical baseline. The gradual increase in current density with increasing potential indicates that Cu^{2+} reduction is limited primarily by diffusional transport to the electrode surface. In the absence of additives, redox processes remain kinetically sluggish due to the lack of charge transfer facilitators. The red line illustrates the system containing potassium chloride, which shows a marked enhancement in current density. This behavior is attributed to the adsorption of Cl^- ions on the steel surface, which reduces the overpotential required for Cu^{2+} reduction and promotes the formation of transient Cu-Cl complexes. These species enhance the mobility of redox-active ions and significantly accelerate copper deposition. In contrast, the blue line corresponds to the system containing trisodium citrate. Here, the current density is noticeably lower than in the KCl-containing solution, as citrate complexes with Cu^{2+} ions, decreasing the concentration of free redox-active species in solution. Additionally, citrate adsorption on the electrode surface forms a partial passivating layer, further limiting mass transfer and hindering electrodeposition. Finally, the green line represents bare annealed steel without any copper coating. Its electrochemical response is lower than the systems with additives, yet slightly more active than the pure $CuSO_4$ condition, indicating modest redox activity and minimal copper-related modification.

Figure 10 presents Tafel curves for annealed steel electrodes immersed in copper sulfate solutions without and with additives. The analysis evaluates corrosion resistance and the efficiency of redox processes associated with each system.

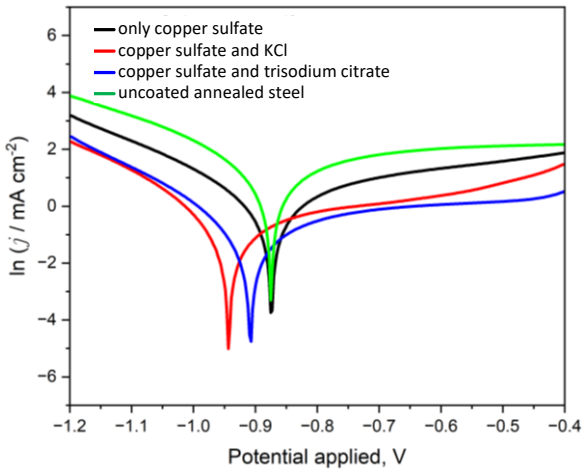

Figure 10. *Tafel curves for the Fe-Cu system in copper sulfate solutions with and without additives (KCl and trisodium citrate). The electrodes were previously electrodeposited at -0.8 V at 120 s*

The black line in Figure 10 corresponds to the system with pure copper sulfate, exhibiting higher charge transfer resistance and lower current densities compared to modified systems. This behavior indicates slow redox kinetics due to the absence of additives that enhance Cu^{2+} mobility. The red line, representing the KCl-containing solution, reveals a substantial reduction in corrosion potential and a marked increase in current density. This improvement arises from Cl^- ion adsorption on the steel surface, which promotes charge transfer by stabilizing transient Cu-Cl complexes and lowering the activation energy barrier. The blue line shows the behavior of the system with trisodium citrate, which acts as a chelating agent, forming stable Cu^{2+} complexes that reduce the availability of free redox-active species. The resulting lower current densities are also influenced by citrate-induced surface passivation, which modulates electrochemical reactivity and promotes a more controlled redox process. Finally, the green line denotes the response of bare annealed steel, showing the lowest current densities due to limited redox activity and minimal surface modification, thus confirming its higher corrosion resistance in the absence of copper coatings.

The Tafel curves confirm that KCl is the most efficient additive for improving charge transfer and reducing the corrosion potential, while trisodium citrate provides passive and uniform control of the redox process. Bare steel serves as a reference, highlighting the inherent electrochemical limitations of the base system.

Figure 11 illustrates the linear sweep voltammetry results for an annealed steel electrode in various copper sulfate solutions, evaluated after copper electrodeposition at -0.6 V.

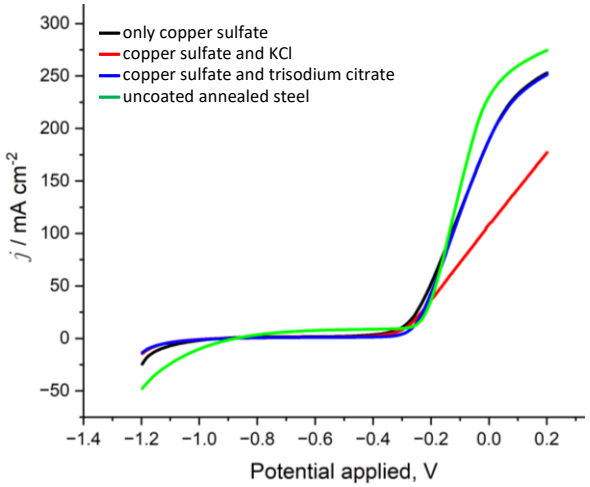

Figure 11. *Linear sweep voltammograms of Fe-Cu system in copper sulfate solutions with and without additives (KCl and trisodium citrate). The electrodes were previously electrodeposited at -0.6 V for 120 s*

Figure 11. Linear sweep voltammograms of Fe-Cu system in copper sulfate solutions with and without additives (KCl and trisodium citrate). The electrodes were previously electrodeposited at -0.6 V for 120 s Pure copper sulfate (black line): The system demonstrates a moderate current response, indicating significant diffusion limitations and charge transfer resistance. This behaviour reflects the absence of additives to facilitate ionic mobility and enhance electrode kinetics. Copper sulfate with KCl (red line): The substantial increase in current density signifies improved charge transfer efficiency, driven by the adsorption of Cl- ions on the electrode surface. These ions stabilize transient Cu-Cl complexes, reducing the activation energy for Cu^{2+} reduction and promoting rapid electron transfer. Copper sulfate with trisodium citrate (blue line): The addition of citrate induces a controlled redox process by forming stable Cu-citrate complexes. These complexes diminish the concentration of free Cu^{2+} ions available for reduction, resulting in reduced current density and enhanced deposition uniformity. Furthermore, the chelation effect modulates charge transfer

dynamics, promoting precise electrochemical behaviour. Annealed steel without treatment (green line): The lowest current density is observed in this system, highlighting minimal electrochemical activity. This behaviour underscores the absence of surface modifications or electrochemical treatments to enhance reactivity or mitigate resistive processes.

This figure underscores the critical role of additives in tailoring the electrochemical performance of annealed steel electrodes within copper sulfate systems, providing insights into optimizing charge transfer and deposition processes.

Figure 12 presents Tafel curves for the Fe-Cu system in different copper sulfate-based solutions, emphasizing the electrochemical changes observed at a lower potential of -0.6 V. Compared to the results at -0.8 V (Figure 10), the reduced overpotential introduces distinct shifts in corrosion behaviour and redox dynamics for each condition.

The green line in Figure 12 represents the uncoated annealed steel, which serves as the baseline and displays minimal redox activity. Its cathodic branch shows low current densities, indicating limited electron transfer, while the anodic branch remains steep, reflecting the inherent passivity of the material. In contrast, the black line, corresponding to the pure copper sulfate system, exhibits increased current densities due to Cu^{2+} participation in redox processes. However, despite a slightly less negative corrosion potential compared to -0.8 V, kinetic limitations persist as the lower overpotential reduces the driving force for Cu^{2+} reduction. The red line shows that the addition of KCl significantly enhances redox efficiency, evidenced by a steeper cathodic slope and higher current density. Chloride ions facilitate charge transfer by stabilizing transient Cu-Cl complexes and lowering activation barriers, making the system effective even under reduced energy input. The blue line, associated with the trisodium citrate system, presents a controlled redox response, where Cu^{2+} chelation limits the concentration of free redox-active species. Although the current density remains below that of the KCl system, it is slightly improved compared to -0.8 V. The continued presence of a passivating layer and balanced deposition kinetics highlights citrate's role in delivering uniform and stable coatings under moderated electrochemical conditions.

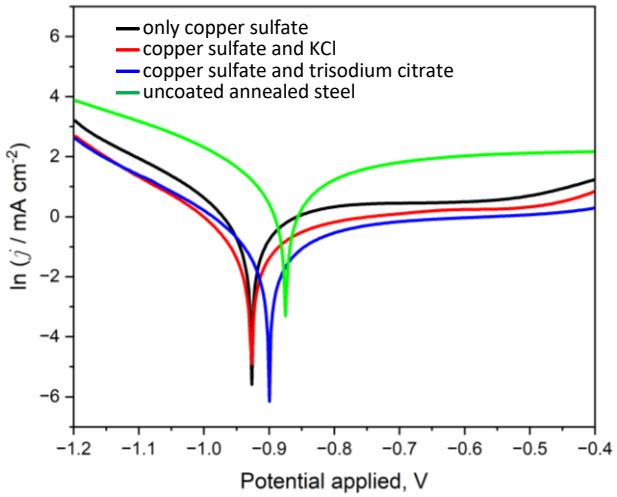

Figure 12. *Tafel curves for the Fe-Cu system in copper sulfate solutions with and without additives (KCl and trisodium citrate). The electrodes were previously electrodeposited at -0.6 V for 120 s*

Table 4 presents the electrochemical parameters obtained through the analysis of Tafel curves, derived from linear sweep voltammetry experiments performed on annealed steel electrodes subjected to varying conditions. These experiments were conducted to evaluate corrosion resistance and redox activity in copper sulfate solutions with and without the inclusion of additives (KCl and

trisodium citrate). Table 4 provides the observed corrosion potential ($E_{corr,obs}$), corrosion current density (j_{corr}), total corrosion current (i_{corr}), corrosion rate (CR) and polarization resistance (R_p). The parameters were calculated using the standard Tafel extrapolation method, revealing the role of the additives and electrodeposition potentials in modulating corrosion behaviour [28,29].

Table 4: *Electrochemical parameters derived from Tafel curve analysis for the Fe-Cu systems*

Electrode system	$E_{corr,\ obs}$ / V	j_{corr} / mA cm^{-2}	i_{corr} / µA	CR, mm year^{-1}	R_p / Ω
Uncoated annealed steel	-0.874	13.33	267.9	154.87	891.71
*Cu electrodeposited (no additives) at -0.8 V	-0.874	2.174	43.7	25.259	2392.6
*Cu electrodeposited (no additives) at -0.6 V	-0.926	3.212	64.6	37.328	2748.6
**Cu electrodeposited with KCl at -0.8 V	-0.942	0.927	18.6	10.768	4968.2
**Cu electrodeposited with KCl at -0.6 V	-0.927	0.692	13.9	8.0455	5402.3
**Cu electrodeposited with citrate at -0.8 V	-0.908	0.725	14.6	8.4201	6246.6
**Cu electrodeposited with citrate at -0.6 V	-0.899	0.751	15.1	8.7259	6319.2

*Electrodes were prepared by electrodeposition using only $CuSO_4$ solutions without additives

**Electrodes were prepared by electrodeposition using $CuSO_4$ solutions with the specified additive (KCl or trisodium citrate).

Uncoated annealed steel: Serving as the baseline system, uncoated annealed steel exhibits high j_{corr} (13.33 mA cm^{-2}) and low R_p (891.71 Ω), reflecting its high susceptibility to corrosion. The absence of protective coatings or additives results in active corrosion processes, as evidenced by the significant corrosion rate (154.87 mm year^{-1}).

Electrodeposited copper from pure $CuSO_4$ at -0.8 and -0.6 V: When the electrodeposition is performed at -0.8 V in pure copper sulfate, the j_{corr} is significantly reduced to 2.174 mA cm^{-2}, leading to a marked decrease in the corrosion rate (25.259 mm year^{-1}) and an increase in R_p (2392.6 Ω). This improvement is attributed to the formation of a metallic copper layer, which acts as a barrier against corrosion. At -0.6 V, the corrosion potential shifts further negative (-0.927 V), indicating greater thermodynamic stability. However, the j_{corr} increases slightly (3.212 mA cm^{-2}), suggesting less efficient passivation due to a thinner or less uniform copper layer.

Electrodeposited copper with KCl additive: Adding KCl to the system at -0.8 V results in the most efficient protection, as reflected by the lowest j_{corr} (0.92667 mA cm^{-2}) and corrosion rate (10.768 mm year^{-1}). The polarization resistance increases significantly to 4968.2 Ω, indicating enhanced charge transfer resistance. This improvement is due to the chloride ions (Cl^-) adsorbing on the electrode surface, stabilizing transient Cu-Cl complexes, and promoting uniform copper deposition. At -0.6 V, the system remains robust, with slightly higher R_p (5402.3 Ω) and lower j_{corr} (0.692 mA cm^{-2}).

Electrodeposited copper with trisodium citrate additive: Trisodium citrate systems exhibit moderate *j*corr values compared to KCl but offer controlled corrosion resistance through surface passivation. At -0.8 V, R_p reaches 6246.6 Ω, the highest among all conditions, indicating effective chelation of Cu^{2+} ions and the formation of a stable protective layer. The slightly lower j_{corr} at -0.6 V (0.75095 mA cm^{-2}) confirms the system's balance between surface protection and redox activity.

These datasets highlight the critical impact of additives (KCl and trisodium citrate) and electrodeposition potential on the Fe-Cu system's electrochemical performance. KCl demonstrates the highest efficiency in reducing corrosion and enhancing charge transfer, as evidenced by the lowest corrosion current densities and highest polarization resistances. Trisodium citrate offers the most controlled deposition and passivation, suitable for applications requiring uniformity and stability over high efficiency. Pure $CuSO_4$ serves as a baseline for understanding the unoptimized behaviour of the system. Uncoated steel reinforces the necessity of coatings or additives to mitigate aggressive

corrosion. These results emphasize the need for precise selection of deposition conditions and additives to tailor electrochemical performance for specific applications. This consideration aligns with findings in related corrosion studies under cathodic protection environments [30].

Conclusions

This study elucidates how KCl and trisodium citrate in cupric sulfate solutions modulate the electrochemical behaviour of steel, specifically by influencing the cathodic copper deposition ($Cu^{2+} + 2e^- \rightarrow Cu^0$) and anodic iron dissolution ($Fe^0 \rightarrow Fe^{2+} + 2e^-$). Key findings are summarized as follows:

Cupric sulfate with KCl: This system demonstrates the highest efficiency in corrosion protection by drastically reducing the corrosion current density and corrosion rate. The highly negative E_{corr} and high polarization resistance confirm its robust electrochemical properties, making it ideal for applications requiring maximum corrosion mitigation.

Cupric sulfate with trisodium citrate: Although less efficient in terms of current density, this system offers precise control of redox processes through the formation of stable Cu-citrate complexes. Its ability to stabilize active species positions it as a suitable choice for systems requiring homogeneous and well-controlled copper deposits.

Pure cupric sulfate: This system shows improvements over bare steel but lacks the protective efficiency observed in systems with additives, underlining the importance of modifiers in optimizing electrochemical performance. Uncoated: Results confirm the high reactivity and susceptibility of unprotected steel to corrosion, emphasizing the necessity of coatings or surface modifications for industrial applications.

In conclusion, the incorporation of additives such as KCl and trisodium citrate represents an effective strategy for optimizing Fe-Cu systems in terms of corrosion protection and modulation of electrochemical activity. These findings have significant implications for the design of advanced technologies in electrodeposition, electrochemical sensors, and cathodic protection systems.

Key insights at both applied potentials (-0.6 and -0.8 V): The KCl system is confirmed as the most efficient for copper electrodeposition, demonstrating optimal electrochemical properties for practical applications. The enhancement in charge transfer and ionic transport promoted by KCl is evident across all evaluated aspects. Trisodium citrate, while less efficient in terms of current density, provides detailed control over the deposition process, which is valuable for applications requiring more uniform and well-defined deposits. Pure copper sulfate highlights its intrinsic limitations, emphasizing the importance of additives to enhance the system's electrochemical properties and overall efficiency. These results collectively underscore the pivotal role of additives in tailoring Fe-Cu systems for specific applications, offering insights into the development of advanced electrochemical technologies. This study focuses on electrochemical dynamics rather than structural characterization; deposit morphology analysis via SEM or AFM is proposed as a future study to complement these findings with structural insights.

Data analysis: *All experiments were performed in triplicate to ensure reproducibility. Data were processed using NOVA 2.1 and OriginPro 2024 software. Parameters for evaluating corrosion kinetics were determined through nonlinear regression fitting to Tafel equations [17].*

Data availability: *All data generated during this study, including voltammograms, Nyquist plots, and chronoamperometric results, are available upon direct request to the author. The chemical solutions and materials used are standard in electrochemical research and present no ethical or availability restrictions.*

***Acknowledgements**: I sincerely appreciate the Universidad Politécnica de Lázaro Cárdenas for offering me the opportunity and the essential resources to carry out this project.*

References

[1] K. Bijapur, V. Molahalli, A. Shetty, A. Toghan, P. De Padova, G. Hegde, Recent Trends and Progress in Corrosion Inhibitors and Electrochemical Evaluation, *Applied Sciences* **13** (2023) 10107. https://doi.org/10.3390/app131810107

[2] Y. V. Ivshin, F. N. Shaikhutdinova, V. A. Sysoev, Electrodeposition of Copper on Mild Steel: Peculiarities of the Process, *Surface Engineering and Applied Electrochemistry* **54** (2018) 452-458. https://doi.org/10.3103/S1068375518050046

[3] A. Pasha, S. Khasim, A. A. A. Darwish, T. A. Hamdalla, S. A. Al-Ghamdi, High Performance Organic Coatings of Polypyrrole Embedded with Manganese Iron Oxide Nanoparticles for Corrosion Protection of Conductive Copper Surface, *Journal of Inorganic and Organometallic Polymers and Materials* **32** (2022) 499-512. https://doi.org/10.1007/s10904-021-02130-x

[4] U. Rocabert, F. Muench, M. Fries, B. Beckmann, K. Loewe, H. A. Vieyra, M. Katter, A. Barcza, W. Ensinger, O. Gutfleisch, Electrochemical Corrosion Study of $La(Fe_{11.6-x}Si_{x1.4}Mn_x)H_{1.5}$ in Diverse Chemical Environments, *Electrochimica Acta* **434** (2022) 141200. https://doi.org/10.1016/j.electacta.2022.141200

[5] G. Vasyliev, V. Vorobyova, D. Uschapovskiy, O. Linyucheva, Local Electrochemical Deposition of Copper from Sulfate Solution, *Journal of Electrochemical Science and Engineering* **12** (2022) 557-563. https://doi.org/10.5599/jese.1352

[6] S. Parida, S. Das, A. Mallik, An Experimental Study of Copper Electroplating by Electrochemical Impedance Spectroscopy (EIS) at Room Temperature, *Materials Today: Proceedings* **66** (2022) 544-547. https://doi.org/10.1016/j.matpr.2022.05.596

[7] M. Elrouby, A. Gelany, H. Saber, Potentiostatic Electrodeposition of Copper, Indium, and Cadmium Sulfides for CO_2 Electroreduction: A Path toward Sustainable Hydrogen Generation, *International Journal of Hydrogen Energy* **91** (2024) 877-892. https://doi.org/10.1016/j.ijhydene.2024.10.190

[8] P. Y. Shevelin, N. G. Molchanova, A. N. Yolshin, N. N. Batalov, Electron Transfer in an Electron-Ion Molten Mixture of CuCl-$CuCl_2$-MeCl (Me = Li, Na, K, Cs), *Electrochimica Acta* **48** (2003) 1385-1394. https://doi.org/10.1016/S0013-4686(03)00005-7

[9] A. Dridi, L. Dhouibi, J. Y. Hihn, P. Berçot, W. Sassi, E. M. Rezrazi, CuZn Electrodeposition in Cyanide-Free Electrolytes: Influence of Citrate/Metal Ratio and pH on Simultaneous Copper and Zinc Reduction Kinetics and Alloy Composition Control, *Journal of The Electrochemical Society* **167** (2020) 062508. https://doi.org/10.1149/1945-7111/ab819b

[10] R. Ghosh, V. Sudha, S. Harinipriya, Thermodynamic Analysis of Electrodeposition of Copper from Copper Sulphate, *Bulletin of Materials Science* **42** (2019) 43. https://doi.org/10.1007/s12034-018-1712-1

[11] D. Grujicic, B. Pesic. Electrodeposition of Copper: The Nucleation Mechanisms. *Electrochimica Acta* **47** (2002) 2901-2912. https://doi.org/10.1016/S0013-4686(02)00161-5

[12] K. G. Schmitt, R. Schmidt, J. Gaida, A. A. Gewirth, Chain Length Variation to Probe the Mechanism of Accelerator Additives in Copper Electrodeposition, *Physical Chemistry Chemical Physics* **21** (2019) 16838-16847. https://doi.org/10.1039/C9CP00839J

[13] J. Xu, W. Ren, Z. Lian, P. Yu, H. Yu, A Review: Development of the Maskless Localized Electrochemical Deposition Technology, *International Journal of Advanced Manufacturing Technology* **110** (2020) 1731-1757. https://doi.org/10.1007/s00170-020-05799-5

[14] P. Ye, Q. Niu, F. Wang, Effect of Electrolyte Composition and Deposition Voltage on the Deposition Rate of Copper Microcolumns Jet Electrodeposition, *Materials Science and Engineering: B* **298** (2023) 116857. https://doi.org/10.1016/j.mseb.2023.116857

[15] G. Jerkiewicz, Applicability of Platinum as a Counter-Electrode Material in Electrocatalysis Research, *ACS Catalysis* **12** (2022) 2661-2670. https://doi.org/10.1021/acscatal.1c06040
[16] Y. Lyu, P. Mollik, A. L. Oláh, D. P. Halter, Construction and Evaluation of Cheap and Robust Miniature Ag/AgCl Reference Electrodes for Aqueous and Organic Electrolytes. *ChemElectroChem* **11** (2024) e202300792. https://doi.org/10.1002/celc.202300792
[17] E. Garcia, J. Torres, N. Rebolledo, R. Arrabal, J. Sanchez, Corrosion of Steel Rebars in Anoxic Environments. Part I: Electrochemical Measurements, *Materials* **14** (2021) 2491. https://doi.org/10.3390/ma14102491
[18] X. Yu, X. Li, G. Zheng, Y. Wei, A. Zhang, B. Yao, Preparation and Properties of KCl-Doped Cu2O Thin Film by Electrodeposition, *Applied Surface Science* **270** (2013) 340-345. https://doi.org/10.1016/j.apsusc.2013.01.026
[19] J. Wang, F. Xie, Y. Pan, W. Wang, Leaching of Gold with Copper-Citrate-Thiosulfate Solutions, *Mineral Processing and Extractive Metallurgy Review* **43** (2021) 916-925. https://doi.org/10.1080/08827508.2021.1969389
[20] J. Peng, B. Chen, Z. Wang, J. Guo, B. Wu, S. Hao, Q. Zhang, L. Gu, Q. Zhou, Z. Liu, S. Hong, S. You. A. Fu, Z. Shi, H. Xie, D. Cao, C.-J. Lin, G. Fu, L.-S. Zheng, Y. Jiang, N. Zheng, Surface Coordination Layer Passivates Oxidation of Copper, *Nature* **586** (2020) 390-394. https://doi.org/10.1038/s41586-020-2783-x
[21] F. Nikkhou, F. Xia, A. P. Deditius, Variable Surface Passivation During Direct Leaching of Sphalerite by Ferric Sulfate, Ferric Chloride, and Ferric Nitrate in a Citrate Medium, *Hydrometallurgy* **188** (2019) 201-215. https://doi.org/10.1016/j.hydromet.2019.06.017
[22] G. S. Sajadi, V. Saheb, M. Shahidi-Zandi, S. M. Ali Hosseini, A Study on Synergistic Effect of Chloride and Sulfate Ions on Copper Corrosion by Using Electrochemical Noise in Asymmetric Cells, *Scientific Reports* **12** (2022) 14384. https://doi.org/10.1038/s41598-022-18317-2
[23] M. Schneider, U. Langklotz, L. Kühne, U. Gierth, Investigation of Anodic Oxide Formation on AA 7075 in Citric Acid, *Materials Chemistry and Physics* **320** (2024) 129458. https://doi.org/10.1016/j.matchemphys.2024.129458
[24] K. R. Cooper, M. Smith, Electrical Test Methods for On-Line Fuel Cell Ohmic Resistance Measurement, *Journal of Power Sources* **160** (2006) 1088-1095. https://doi.org/10.1016/j.jpowsour.2006.02.086
[25] O. Gharbi, A. Dizon, M. E. Orazem, M. T. Tran, B. Tribollet, V. Vivier, From Frequency Dispersion to Ohmic Impedance: A New Insight on the High-Frequency Impedance Analysis of Electrochemical Systems, *Electrochimica Acta* **320** (2019) 134609. https://doi.org/10.1016/j.electacta.2019.134609
[26] A. Dutta, J. Kaur, A. Saxena, Boosting the Corrosion Inhibition Efficiency of the *Clerodendrum serratum* Extract for Steel in the Presence of KCl, *Chemical Data Collections* **52** (2024) 101148. https://doi.org/10.1016/j.cdc.2024.101148
[27] M. Chahbi, A. Mortadi, S. Zaim, N. El Ghyati, M. Monkade, R. El Moznine, A New Approach to Investigate the Ionic Conductivity of NaCl and KCl Solutions via Impedance Spectroscopy, *Materials Today: Proceedings* **66** (2022) 205-211. https://doi.org/10.1016/j.matpr.2022.04.489
[28] J. Roscher, D. Liu, X. Xie, R. Holze, Comparative Assessment of Aromatic Iron Corrosion Inhibitors with Electrochemical Methods, *Corrosion and Materials Degradation* **5** (2024) 593-600. https://doi.org/10.3390/cmd5040027
[29] F. A. Nuñez Pérez, Electrochemical Analysis of Corrosion Resistance of Manganese-Coated Annealed Steel: Chronoamperometric and Voltammetric Study, *AppliedChem* **4** (2024) 367-383. https://doi.org/10.3390/appliedchem4040023

[30] M. G. R. Mahlobo, P. A. Olubambi, P. Mjwana, M. Jeannin, P. Refait, Study of Overprotective-Polarization of Steel Subjected to Cathodic Protection in nsaturated Soil, *Materials* **14** (2021) 4123. https://doi.org/10.3390/ma14154123